A Simple and Accurate Computation Method of Stator End-Winding and Rotor End-Ring Parameters of Induction Machines

A. Saidoune [*1,2], H. Houassine [1,2], S. Bensaid [1,2], N. Yassa [1,2], F O. Serteller [3],

[1] Faculty of Sciences and Applied Sciences, Bouira University, Algeria,

[2] Laboratory of Materials and Sustainable Development (LMDD) Bouira, Algeria.

[3] Electric-Electronic Engineering Department, Technology Faculty, Marmara University, Türkiye.

(Corresponding Author): *E-mail: a.saidoune@univ-bouira.dz

Received: 01-05-2023 **Accepted:** 17-05-2023 **Published:** 31-05-2023

Abstract

This paper proposes a new method to accurately estimate the inductances and resistances of a three-phase squirrel cage induction motor. It is based on low voltage impedance measurement and calculation using a 2D finite element model combined with circuit equations. The short-circuit ring inductance and resistance are determined using an inverse problem technique, which involves the iterative solution of a magneto-harmonic model. The proposed technique is validated by introducing the obtained parameters into the 2D-FE model with nominal operating conditions, confirming its accuracy and reliability.

Keywords: Parameter identification, Stator end winding, Rotor short-circuit ring, Impedance measurement

Tob Regul Sci. ™ 2023;9(1): 1946-1961
DOI: doi.org/10.18001/TRS.9.1.134

I- Introduction:

The asynchronous motor is the most widely used drive-in industry [1]. The analysis and diagnosis of these motors generally require analytical or numerical simulations, which consist in solving the mathematical equations expressing the multi-physical behaviour of the machine [2]. For an accurate simulation of asynchronous motors, it is necessary to predetermine the parameters of the windings, which are essential elements of the equivalent electrical circuits of these motors [3]. These parameters can be classified into two distinct categories. The winding's active parts parameters are located insidethe slots or simply inside the saturable magnetic regions. The end windings parameters are located in the air (the non-saturableareas) [1,3]. The stator end winding (stator coil heads) and rotor short-circuit rings belong to the second category; their

resistances and inductances influence the overall behaviour and performance of the squirrel cage induction motor [4].Precisely determining there is a very delicate and unavoidable task[2, 4].

Several works in the literature have focused on calculating and estimating these parameters[3].The stator end winding and rotor shorting rings calculation parameters can be done using analytical formulations as mentioned in the works [5,6,7,8] and 3D numerical calculation developed by [8,9,10]. In addition, several comparative studies have been performed by [11,12], confirming the advantages and disadvantages of these methods. [13,14,15]

This paper proposes a new approach for accurately estimating the resistances and inductances of the stator coil heads and rotor short-circuit rings of the three-phase squirrel cage induction motor. The methodfocuses primarily on measuring the impedance at low voltage (below 2V) and the ambient temperature of a stator phase simultaneously in the absence and presence of the unitary slip rotor. The method is associated with a 2D finite element model coupled to the circuit equations, implemented in MATLAB, with which the impedance is calculated successively for the two considered cases, Short-circuit rings and stator coil heads.

At first, the impedance of a stator phase expresses the inductance and resistance of the active part of the stator winding and its extremities (coil heads)measuring without a rotor. In the finite element model, the coupling circuit considers both the functional components and the ends. Thestator end winding inductance and resistance are determined from the simultaneous measurement and calculation of the impedance without a rotor. These parameters are then introduced into the finite element model to determine the short circuit ring parameters.

Secondly, the measurement in the presence of the rotor is carried out, and the measured impedance of a stator phase contains all the resistances and inductances of the stator and rotor windings (squirrel cage). The finite element model takes the active parts of these windings into account. The ends of these windings are supported in the circuit coupling by adding resistive and inductive components with constant values. The inverse problem technique is used to determine the inductance and resistance of the short-circuit ring portions of the squirrel cage induction motor. This technique requires an iterative solution of the magneto-harmonic model described by the FE with the minimisation of a cost function that expresses the difference between the measured impedance and the one calculated by the FE model [16, 17, 18].The minimisation of

the cost function is done by the Nelder-Mead simplex method. The convergence is ensured, whatever the initial values of the inductance and resistance of the short-circuit rings[20]. We used the parameters obtained through the inverse problem technique (i.e., resistance and inductance of the coil heads and the short-circuit ring) to validate the proposed technique in a finite element model. We supplied the model with a nominal voltage and used it to determine the main operating characteristics of the asynchronous motor.

2- Presentation of the proposed method

The proposed method is based on two experimental tests at low voltage (less than 2V) 50Hz, which allow the measurement of the impedance of one stator phase (the other phases are open) of the machine using an LCRMeter. The first test is performed without the rotor and the second with the unitary slip rotor. All tests are performed at ambient temperature. Once both tests are completed, the inverse model uses the measured parameters. The latter consists of calculating the impedance one or more times by a 2D-FE model (Direct Model), expressing precisely each test, and modifying the desired parameters (inductances and coil end resistances) each time. Identifying the inductance and resistance of the coil ends requires a single iteration of impedance calculation by the FE model, with initial values of the inductance and resistance of the coil ends at zero. The difference between the measured and calculated inductance gives the coil-head inductance of a stator phase, and it is the same for the resistance of the stator coil ends. Identifying the inductance and resistance of the short-circuit ring portions requires several iterations of impedance calculation by the FE model with any initial values of the inductance and resistance of the short-circuit ring portions. The calculated impedance is compared with the measured impedance at each iteration. The obtained short circuit ring parameters are those given the slightest difference (imposed tolerance) between the measured and calculated impedances of the stator phase.

The technique for calculating the coil-head parameters involves estimating stator coil-head inductance using measurements and values obtained by resolving the 2D-FE model

model of the machine without a rotor. The stator heads coil inductance and resistance are deduced from the numerical difference between the total inductance value measured from the test without a rotor and the one calculated from the 2D-FE model, where the parameters of the coil heads to be identified are initially neglected. The parameters thus identified are injected into the numerical model without a rotor, and the new value of the calculated inductance is validated by comparison with the experimentally measured one. The obtained parameters of the coil heads are introduced into the machine's 2D-FE model in the rotor's presence. The inductance and resistance of the short circuit ring Lring, andRring,respectively, are initialised to a random value. The identification of the short circuit ring parameters is performed using a Simplex inversion algorithm which is detailed in

subsection 2.3. Those parameters are validated by comparing the experimental and the numerical results. Once the required parameters are identified, the obtained results from the complete numerical model are validated by comparison with those given by the constructor.

The proposed technique involves estimating the stator coil-head inductance using measurements

without a rotor and the values obtained from resolving the 2D-FE model of the machine without a rotor to calculate the coil-head parameters. The stator heads coil inductance and resistance are deduced from the numerical difference between the total inductance value measured from the

test without a rotor and the one calculated from the 2D-FE model, where the parameters of the coil heads to be identified are initially neglected. The parameters thus identified are injected into the numerical model without a rotor, and the new value of the calculated inductance is validated by comparison with the experimentally measured one.

2.1- Experimental measurement bench

The experimental bench shown in Figure 1.a and 1.b is used to measure the machine without a rotor and the machine with a rotor, respectively, to carry out the abovementioned measurements. Using a precise LCRMeterfrom GWinstek

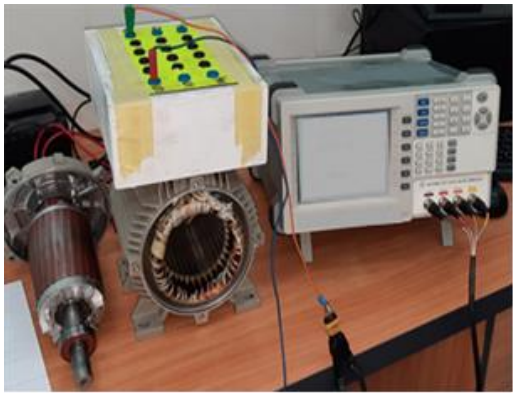

Figure 1.a: Testing without the rotor

The test bench consists of an LCR_meter and a squirrel-cage induction motor. The squirrel-cage induction machine tested is of 1.5kW power (produced by Electro-Industries, Azazga, Algeria), whose manufacturer's characteristics are given in Table 1.

Characteristic	Value	Unit
Brand	ENEL	-
Power output	1.5	kW
Number of phases	3	-
Supply frequency	50	Hz
Supply voltage	230/400	Volt
Current consumption	5.97/3.45	Ampere
Coupling	Y/ Δ	-
Number of poles	4	-
Speed	1410	Rpm

Table 1: Machine characteristics according to the nameplate

Measurements are made on all three phases for both configurations with and without rotor measurements. The phase concerned by the measure is supplied separately from the other two phases via a precision LCR_meter (GWinstek LCR8105G) under a low 50Hz sinusoidal voltage (less than 2V),as shown in Fig. 2.

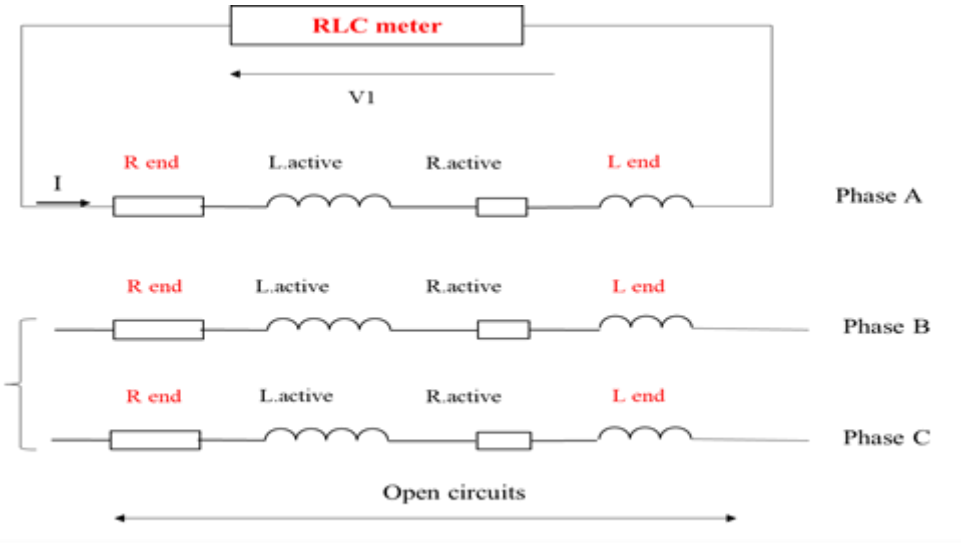

Figure 2: experimental measurement scheme

The following formula gives the voltage of the phase concerned by the measurement:

$$U = (R_{active} + R_{end})I + (L_{active} + L_{end})\, j\omega_s I \qquad (1)$$

Where:

$R_{active} + R_{end}$ and $L_{active} + L_{end}$ are the total resistance and inductance of the phase.

Table 2 summarises eachmeasured phase inductance and resistance value using the LCRMeter.

Table 2: Measurement of stator resistances and inductance using LCRMeter

	Rph [Ohm] measured	Lph [mH] measured
Without rotor	6.177	18.21
With rotor	9.063	27.27

2.2- 2d-finite element model of the studied machine:

Like any electrotechnical device, the asynchronous machine can be modelled using the finite element method, which involves dividing the study domain into finite elements to solve the partial differential equations of the machine model derived from Maxwell's equations, the behaviour laws, and boundary conditions [21]

The magneto-harmonic formulation coupled with electrical circuit equations of the studied problem using the potential vector A is given by (2)

$$\nabla \cdot \left(v\vec{\nabla}\vec{A}\right) = \sigma\left(\frac{\partial \vec{A}}{\partial t} + \vec{\nabla}V\right) - \vec{J_s} \qquad (2)$$

In the harmonic mode, this equation becomes:

$$\nabla \cdot \left(v\vec{\nabla}\vec{A}\right) = \sigma\left(j\omega\vec{A} + \vec{\nabla}\,\mathrm{V}\right) - \vec{J_s} \qquad (3)$$

Where:

A– is the potential magnetic vector,

V– is scalar electrical potential,

Js– is the current density vector,

υ– is the magnetic reluctivity,

σ– is the electrical conductivity.

For the pre-processing step of the 2D-FE analysis, the geometrical model, the physical properties of the materials and the coupled circuit are required. The boundary conditions must be established with a geometric model. A rotating air gap and coupled electrical circuits are applied. The circuit model is coupled with the magneto-harmonic model using the following equation:

$$U_s = R_s I_s + L_{\_end}\frac{d}{dt}I_s + L_{\_sp}\frac{d}{dt}I_s \qquad (4)$$

Where:

U_s– is the vector of voltages across the stator phases,

I_s– is the currents vector of the stator phases,

R_s– is the stator resistance matrix,

L_{end}– is the coil head inductances matrix,

L_{sp}– is the main inductances matrix of the three phases.

The main flux of a phase can then be related to the magnetic vector potential, '*A*.' by the following equation:

$$L_{sp}\frac{d}{dt}I_s = \Phi_{sp}(t) = n_s\frac{l}{s}\iint A(t)\,ds \qquad (5)$$

Where:

ns –number of turns per phase, *l*– the effective length

s–thetotal area of the stator conductors.

Using the above expression, the following stator circuit equation, coupled with the magnetic quantities, is obtained:

$$U_s = R_s I_s + L_{end}\frac{d}{dt}I_s + \left[n_s \frac{l}{s}\iint A(t)\, ds\right] \quad (6)$$

For the rotor, the electromagnetic formulationusingthe potential magneticvector is:

$$\nabla\left(\frac{\mathbf{1}}{\boldsymbol{\mu}}\nabla \cdot \vec{A}\right) - \sigma\left(j\omega_r \vec{A} + \nabla V\right) = \vec{J} \quad (7)$$

Ifthe skin effect in the squirrel cage bars is neglected, the voltage across anelementary bar i can be calculated from the potential magneticvector A using equation (7):

$$[U_i^r] = R_b I_i^r + \frac{l}{s_c}\iint_{sb} j\omega_r \vec{A}\cdot n \cdot ds \quad (8)$$

Where:

I^r_i– is the current in the elementary bar *I*, *sb* and *l* are the section and the length of the bar i, respectively.

The discretised form of equation (8) by the finite element method is given by

$$[U_i^r] = R_b I_i^r + \frac{l}{s_b}\sum_{e=1}^{n_{ei}}\left[\frac{s^e}{3}\sum_{p=1}^{3}\left(j\omega_r A_p^e\right)\right] \quad (9)$$

Where:*l*, n_{ei} describes the mesh elements of the i bar.

The solving of thestudied machine is performed using MATLAB software. Figure (3) illustrates the response of the stator and rotor laminations to magnetic fields. This curve shows saturation for values of the magnetic induction B close to 2 Tesla.

For identifyingR_{end}, L_{end} and R_{ring}, L_{ring}, the linear part of the magnetisation curve is only used because the measurement tests are performed for low voltages. Figure (3)shows the used part of the *B(H)* curve. However, the non-linearity of *B(H)* curve is considered in the nominal mode validation tests of the studied machine.

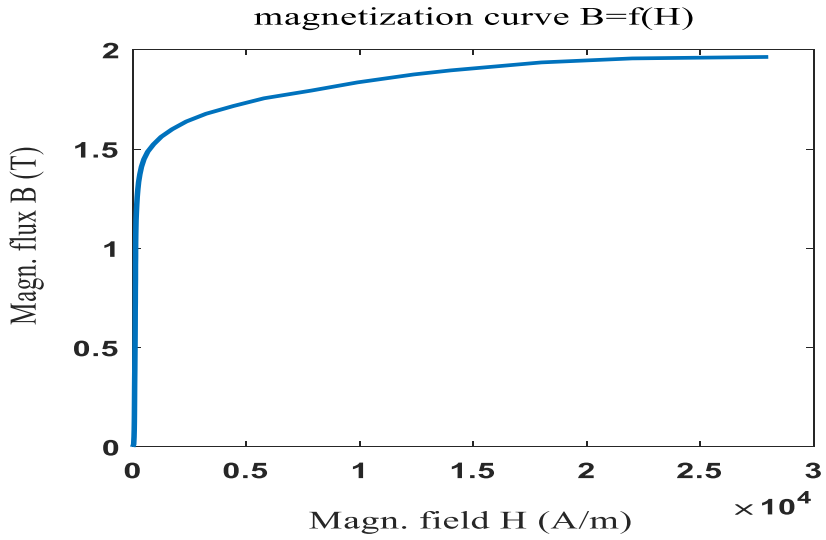

Figure 3: the magnetic circuit Magnetisation curve B=f(H)

The geometrical characteristics of the stator and rotor given by the manufacturer are shown in Table 3.

Tableau 3: stator and rotor geometrical characteristics

Geometrical dimensions	Value	Unit
The outer radius of the stator	135	mm
Stator yoke inner radius	82.5	mm
The outer radius of the rotor	82	mm
Air gap width	0.25	mm
Shaft radius	37.5	mm

The machine finite element model is made using the given manufacturer's characteristics under Matlab software to:

Analyse the evolution of the output quantities of the machine for a unit value of the slip.

Study the magneto-harmonic behavior of the machine supplied by a small 50Hz sinusoidal single-phase voltage source (less than 2V).Fig.4 illustrates the shapes and dimensions of the stator and rotor slots given by the manufacturer.

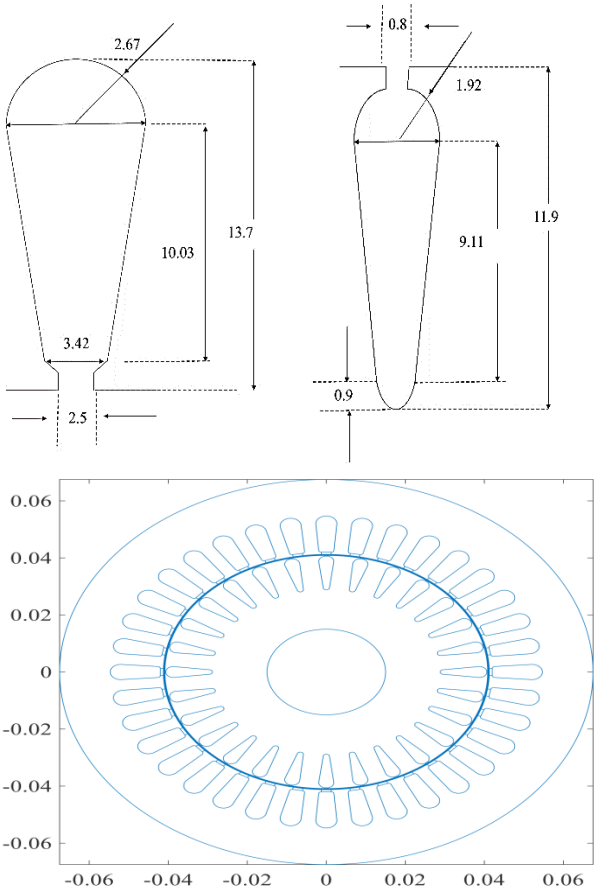

Figure 4.a. Dimensions of stator and rotor slotsFigure 4.b. Shapes of stator and rotor slots

2.3 - Parameters identification

Fig.1 illustrates the stator scheme;R_{end}, L_{end} represents the resistance and inductance of the stator winding coil heads. Fig. 5 shows the electrical diagram of the squirrel cage of the machine, where Rring and Lring are the resistance and inductance of the short circuit ring. Thestudied machine parameters (R_{end}, L_{end} and R_{ring}, L_{ring}) are identified by two successive steps.

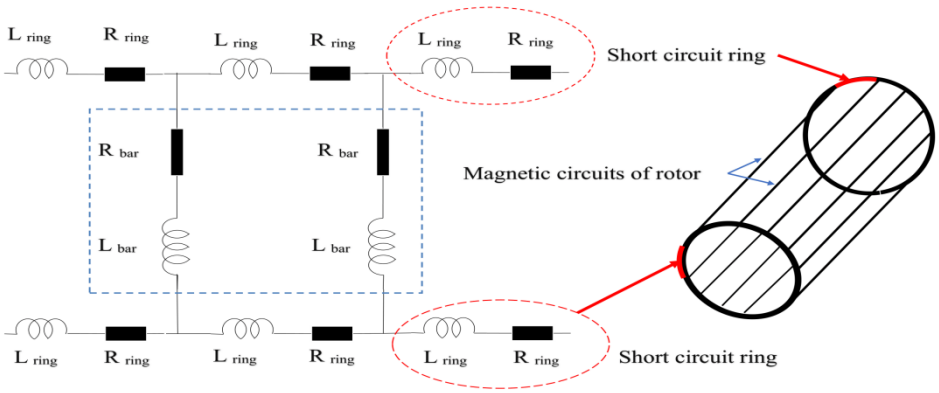

Figure 5: electrical diagram of the rotor squirrel cage

In the first step, the inductance and resistance of the stator winding heads coil are determined by simultaneous measurement and calculation of the impedance without a rotor.In this case, experimentally measured impedances represent the inductance and resistance of active parts and coil heads of the stator.The 2D-FE model can only calculate the impedance of the active region. However, the heads coil of these windings is supported in the electrical coupling circuit by adding resistive and inductive components with constant values, initially declared as zero.The difference between the measured and calculated values gives the exact value of the inductance and resistance of the stator phase coil ends.

In the second step, the rotor short-circuit rings inductance and resistance are determined using the simultaneous measurement and calculation of the stator phase impedance with a rotor incorporated. In this case, the measured impedance of a stator phase contains all resistances and inductances of the stator and rotor windings (squirrel cage). The active parts of these windings are taken into account by the finite element model. The parameters of the stator coil heads identified in the first step are also inserted in the finite element model of the machine. To determine the inductance and resistance of the squirrel cage short-circuit ring, an iterative inverse problem technique minimises a cost function that expresses the difference between the measured impedance and that calculated by the FE model.The minimisation of the cost function is done by the Nelder-Mead simplex method. Convergence is ensured, whatever the initial values of the inductance and resistance of the short-circuit rings.

2.4. **Inverse problem algorithm**

To determine the inductance and resistance of the short-circuit ring of the squirrel cage, the Nelder-Mead simplex algorithm is used,the cost function that expresses the difference between the measured impedance and the one calculated by the FE model.

2.5. Optimisation algorithm

A general simplex's vertices are the foundation for the Nelder-Mead minimisation method. The simplex is altered by the reflection, expansion, and contraction operations, replacing the vertex with the highest cost function value with a point with a lower value (Nelder & Mead, 1965). Using the SIMPLEX algorithm's probabilistic iterative technique enables a directed exploration of feasible solutions while

minimising error through the inverse problem technique [20]

2.6. Objective function

The inverse problem technique aims to determine the rotor short circuit ring impedance accurately. The stator coil heads inductance and resistance are calculated as explained in section2.3 and introduced into the machine finite element model.To accurately determine the rotor short circuit ring impedance, the stator coil heads inductance and resistance are calculated

as explained in section 2.3 and introduced into the machine finite element model.The 2D-FE model only considers the flux of the active part of the machine. However, the leakage flux due to the rotor end (short circuit rings) inductances is considered in the electrical coupling circuit with random initial values.The measured phase impedance with the incorporated rotor is compared to that calculated by the FE model using the SIMPLEX algorithm. It iteratively modifies the solution until the imposed tolerance of the objective function is satisfied.

In order to determine the short circuit ring parameters (resistance and inductance), the stopping criterion imposed is the tolerance of the objective function, which is the error between the estimated and measured parameters. The convergence is ensured, whatever the initial values of the resistance and inductance of the short-circuit rings[22,23,24].

The objective function (OF) is written as follows:

$$\mathrm{OF} = \frac{1}{2} \times \sqrt{\left(\frac{R_{mes}-R_{cal}}{R_{mes}}\right)^2 + \left(\frac{L_{mes}-L_{cal}}{L_{cal}}\right)^2} \qquad (10)$$

R_{mes}: machine resistance measured by LCRMeter

R_{cal}: machine resistance calculated by 2D-FEmodel

L_{mes}: inductance of the machine measured by LCRMeter

L_{cal}: inductance of the machine calculated per 2D-FEmodel

Fig.8 shows the flowchart of the inversion algorithm to identify the short-circuit ring parameters.Fig.9 shows the evolution of the tolerance of the objective function; as we can see, the convergence is reached after 49 iterations with a low error value of 10^{-7}

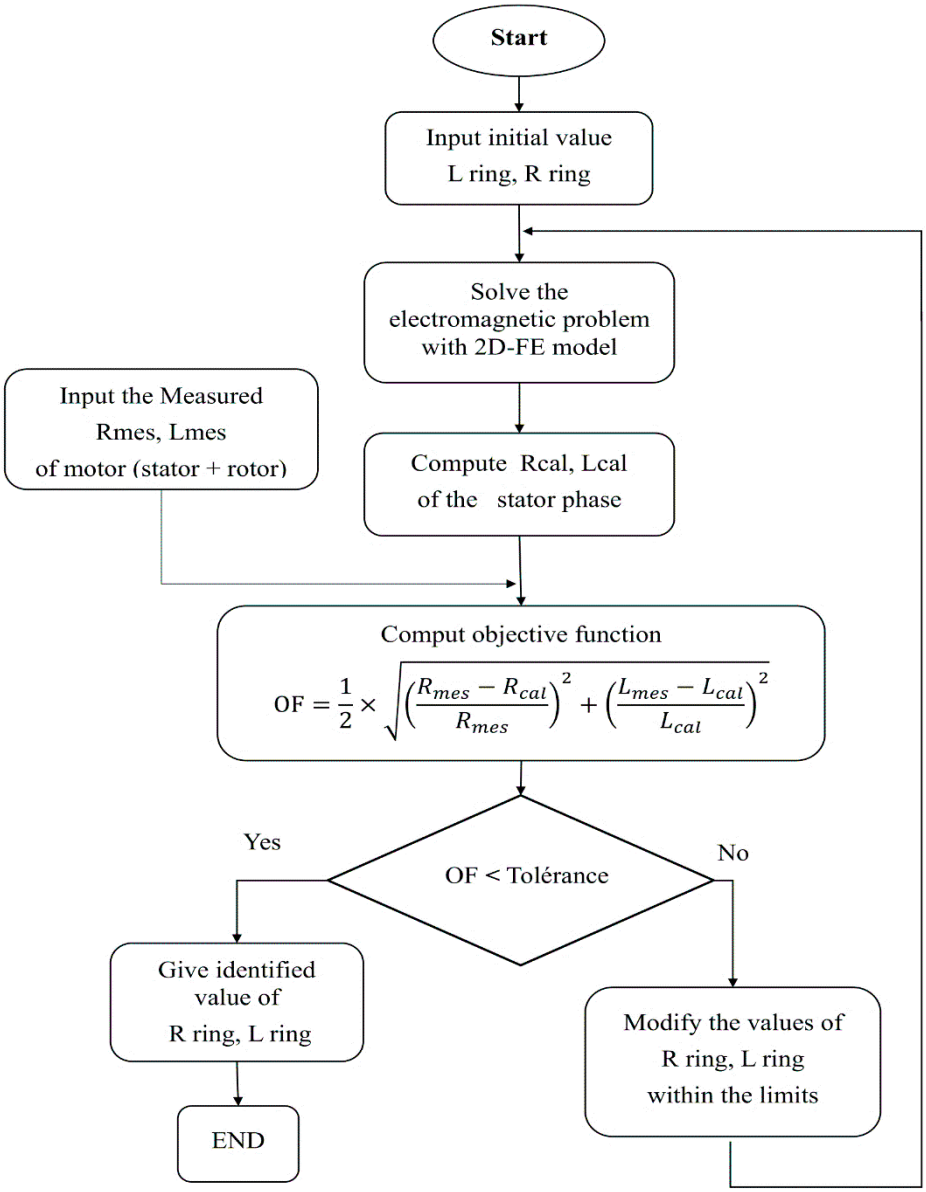

Figure 6: Flowchart of the inversion algorithm

3- Results and discussion

Table 2 shows the values of the parameters Rph Lph measured with theLCRMeter in both cases.Table4 summarises the obtained results for both considered cases. The experimental results are compared with the numerical calculation results.

In the case of the motor without a rotor, the measured values are identical to those estimated.

For the motor with a rotor, the machine's measured phase resistance and phase inductances are 9.063Ω and 27.27 mH and those calculated are 9.0655 Ω and 27.2897 mH with an estimation error of 2.76×10^{-2} and 7.22×10^{-2} respectively which confirms the accuracy of the proposed

method. At the end of this study, the values of the researched parameters, including the resistances and inductances of the stator coil heads and rotor short circuit rings, are summarised in the table below.

Table 4: Identification results

<table>
<tr><td rowspan="7">Without rotor</td><td colspan="2">R end-coil [Ohm]</td><td colspan="2">L end-coil [mH]</td></tr>
<tr><td colspan="2">3.6975</td><td colspan="2">2.334</td></tr>
<tr><td colspan="2">Rph [Ohm]</td><td colspan="2">Lph [mH]</td></tr>
<tr><td>measured</td><td>calculated</td><td>measured</td><td>calculated</td></tr>
<tr><td>6.177</td><td>6.177</td><td>18.21</td><td>18.21</td></tr>
<tr><td colspan="4">Error [%] = (| measured-calculated |/ measured) x 100</td></tr>
<tr><td colspan="2">0.00</td><td colspan="2">0.00</td></tr>
<tr><td rowspan="7">With rotor</td><td colspan="2">Ran [Ohm]</td><td colspan="2">Lan [mH]</td></tr>
<tr><td colspan="2">2.028x10-6</td><td colspan="2">3.2175 x10-6</td></tr>
<tr><td colspan="2">Rph [Ohm]</td><td colspan="2">Lph [mH]</td></tr>
<tr><td>measured</td><td>calculated</td><td>measured</td><td>calculated</td></tr>
<tr><td>9.063</td><td>9.0655</td><td>27.27</td><td>27.2897</td></tr>
<tr><td colspan="4">Error [%] = (| measured-calculated |/ measured) x 100</td></tr>
<tr><td colspan="2">2.76x10-2</td><td colspan="2">7.22x10-2</td></tr>
</table>

3.1- Performance study and validation

In order to validate the proposed technique, the identified parameters (resistances and inductances of the coil heads and the short-circuit ring) using the proposed method are introduced into a finite element model. The simulation of the machine is carried out with a nominal voltage supply to determine the main operating characteristics of the motor.

Table 5 shows the nominal characteristics of the machine obtained by numerical calculation and those given by the manufacturer.As seen, the obtained results confirm the accuracy of the proposed approach for determining the coil head and the short circuit ring parameters. The relative differencebetween the calculated machine principal characteristics and those given by the manufacturer does not exceed 6%.

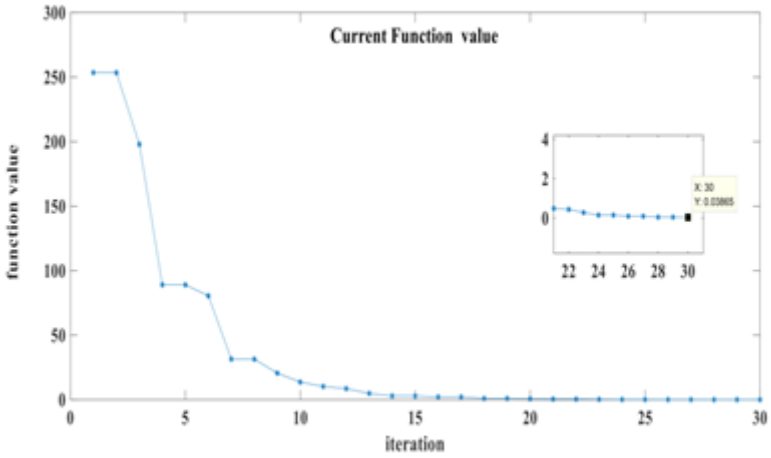

Figure 7: objective function tolerance

Table 5: Main motor characteristics

	Catalogue	Calculated	Error
Nominal slip	0.06	0.06	0.00
Rated current per phase (In) [A]	3.450	3.513	1.826
Rated starting current (Id) [A]	18.285	17.51	4.23
In/Id	5.3	4.984	5.96
Rated torque (Cn) [N/m]	10.000	10.055	0.55
Starting torque (Cd) [N/m]	23.00-25.00	25.515	2.06
Cn/Cd	2.30-2.50	2.55	2.06
Maximum torque (Cmax)	26.00-29.00	29.05	0.17
Cn/Cmax	2.60-2.90	2.905	0.17
Power factor	0.82	0.816	0.49
Efficiency	0.77	0.7747	0.61

4- Conclusion

This paper presents a new approach to accurately measuring the resistances and inductances of the stator coil heads and rotor shorting rings of the three-phase squirrel cage induction motor.The method is mainly based on measuring the stator phase impedance under low sinusoidal voltage (less than 2V) at ambient temperature successively without a rotor and with the presence of a rotor. The method is associated witha 2D finite element model coupled with the electrical circuits, implemented in MATLAB software.In order to validate the proposed technique, the identified parameters (resistances and inductances of the coil heads and the short-circuit ring) are introduced into the finite element model with a nominal voltage supply to determine the main operating characteristics of the motor. The comparison between the calculated characteristics and those given by the manufacturer confirms the accuracy and reliability of the proposed approach.

References

1. Ustinov DA & Garipov BI. " Modelling of induction motor incorporating magnetic saturation" In: Journal of Physics: Conference Series. IOP Publishing 2021: pp.012-017.
2. Schuhmann T, Conradi A, Deeg C, and Brandl K. Determination of stator end winding inductance of large induction machines: comparison between analytics, numerics, and measurements. Electric Power Components and Systems 2013; 41(14): 1397-1414. doi: 10.1080/15325008.2013.821690
3. Amaral GFV, Baccarini JMR, Coelho FCR and Lane MR. A high-precision method for induction machine parameters estimation from manufacturer data. IEEE Transactions on Energy Conversion 2020; 36 (2): 1226-1233.
4. Solodkii, E. M., D. A. Dadenkov, and A. M. Kostygov. "Parametric identification of an induction motor based on a phase-locked-loop frequency control algorithm." Russian Electrical Engineering 89 (2018): 670-674.
5. Ahmed F & KAR NC. Analysis of end-winding thermal effects in a totally enclosed fan-cooled induction motor with a die-cast copper rotor. IEEE Transactions on Industry Applications, 2017. 53(3): 3098-3109.
6. Silberberger M, Morisco DP, Rapp H and Mocke A. Calculation of end-winding leakage inductance for hairpin winding high power density traction machines using the PEEC method. In: IEEE International Electric Machines \& Drives Conference (IEMDC). IEEE, 2021. pp.1-7.
7. Williamson S. and Mueller M A. Calculation of the impedance of rotor cage end rings. In: IEE Proceedings B (Electric Power Applications). IET Digital Library, 1993. pp. 51-60.
8. Lin R \& Arkkio A. Calculation and analysis of stator end-winding leakage inductance of an induction machine. IEEE Transactions on Magnetics. 2009. 45(4).
9. Dorrell DG. Calculation and effects of end-ring impedance in cage induction motors. IEEE transactions on magnetics 2005; 41(3):1176-1183. doi: 10.1109/TMAG.2004.843337
10. Zhu E, Liang Y, Han X, Bian X, and Wang C. New analytical algorithm for calculating the end leakage magnetic field of a 300mvar synchronous condenser under no-load condition. IET Electric Power Applications 2021; 15(12): 1564-1573. doi :10.1049/elp2.12121
11. Asad B, Vaimann T, Kallaste A, Rassõlkin A Et Al. Winding function-based analytical model of squirrel cage induction motor for fault diagnostics. In: 26th International Workshop on Electric Drives Improvement in Efficiency of Electric Drives (IWED). IEEE 2019; pp. 1-6.
12. Aragon-Verduzco DA, Escarela-Perez R, Olivares-Galvan JC, Campero-Littlewood E, Maximov S, Et Al. Numerical simulation of a squirrel cage motor including magnetic wedges and radial vents. Ingeniería Investigación Y Tecnología 2021;22(4). doi:10.22201/fi.25940732e.2021.22.4.025

13. Zidat F, Lombard P, Marion F, Soualmi A. Squirrel Cage End Ring Impedance Determination and Its Motor Performances Influence Analysis Using Finite Elements. ISEF. 17th International Symposium on Electromagnetic Fields in Mechatronics, Electrical and Electronic Engineering, Spain 2015.
14. Arshad WM., Lendenman H, Persson H. End-winding inductances of MVA machines through FEM computations and IEC-specified measurements. IEEE Transactions on Industry Applications 2008; 44(6): 1693-1700.
15. Rezaeealam B. Calculation of magnetising and leakage inductances of induction machine using finite element method. Electrical Engineering 2021; 103(1): 315-323. doi:10.1007/s00202-020-01082-8
16. Ferreira RS, and Ferreira AC. End-windings modeling to study transient voltage distribution in machine stator windings using finite element method. The International Conference on Power Systems Transients (IPST2019) in Perpignan. France. 2019.
17. Arjona MA, Castañeda A, Sellschopp FS, Hernández C, Vargas R, et all. An experimental approach to determine end-parameters for a 2D-FE induction motor model. In: 18th International Conference on Electrical Machines. IEEE 2008; p. 1-5.
18. DE Weerdt R, Hameyer K, and Belmans R. End ring inductance of a squirrel-cage induction motor using 2d and 3d finite element methods. In: IAS'95. Conference Record of the 1995 IEEE Industry Applications Conference Thirtieth IAS Annual Meeting. IEEE 1995; pp. 515-522.
19. Lombard P and Zidat F. Determining end ring resistance and inductance of squirrel cage for induction motor with 2D and 3D computations. In: 2016 .22nd International Conference on Electrical Machines (ICEM). IEEE 2016; pp. 266-271.
20. Nelder JA \& Mead R. A simplex method for function minimisation. The computer journal 1965; 7(4):308-313
21. Belsky IO, Kupriyanov IS \& Lukyanov AV. Finite element modeling of asynchronous electric motors with electrical defects of stator and rotor. In Journal of Physics: IOP Publishing 2020; 1680(1):012005. doi:10.1088/1742-6596/1680/1/012005
22. Hameyer K \& Belmans R. Numerical modelling and design of electrical machines and devices. WIT press 1999;